

**REVIEW OF AERONAUTICAL FATIGUE
INVESTIGATIONS IN JAPAN
DURING THE PERIOD JUNE 2017 TO MAY 2019**

Edited by

Shigeru Machida

Takao Okada

Japan Aerospace Exploration Agency

For Presentation at the 36th Conference of
the International Committee on Aeronautical Fatigue and Structural Integrity

Krakow, Poland, 3-4 June, 2019

CONTENTS

	page
<u>1. INTRODUCTION</u>	4
<u>2. FATIGUE AND FAILURE IN METALLIC MATERIALS AND COMPONENTS</u>	
2.1 Fatigue Characteristic of Linear Friction Welded Ti-6Al-4V Joints	6
2.2 Interaction between High- and Low-cycle Thermo-mechanical Fatigue Loadings in Small Crack Growth around Cooling Hole in A Ni-based Superalloy	8
2.3 Fatigue Life and Fatigue Crack Growth Behavior of Non-through Cracks in Friction Stir-Welded 2024-T3 Aluminum Alloy	9
<u>3. FATIGUE AND FAILURE IN COMPOSITE MATERIALS AND COMPONENTS</u>	
3.1 Ply Curving Termination to Suppress Delamination in Composite Ply Drop-Off	11
3.2 Very High-Cycle Fatigue Characteristics of Cross-Ply CFRP Laminates in Transverse Crack Initiation	13
3.3 Damage mechanisms and mechanical properties of directly bonded CFRTP and aluminum with nano-structured surface	14
3.4 Tensile Test of Ti/CFRP Scarf Joint with One Stringer	15
<u>4. STRUCTURAL HEALTH MONITORING</u>	
4.1 Flight testing of an ultrasonic based SHM system	16
4.2 Real-time Stress Concentration Monitoring of Aircraft Structure during Flights using Optical Fiber	

Distributed Sensor with High Spatial Resolution	17
4.3 Optical Fiber Sensor based Impact Detection System for Aircraft Structures	19
4.4 Reconstruction of Local Stress Field using Strain Monitoring Data	21

5. FULL SCALE TESTING

5.1 Full Scale Fatigue Testing for Mitsubishi Regional Jet	23
5.2 Research on Lightweight Airframe Structure	25

6. MISCELLANEOUS

6.1 Lightning Strike Damage of CF/epoxy Composite Laminates with Conductive Polymer Layers	26
6.2 Effect of Plate Thickness and Paint on Lightning Strike Damage of Aluminum Alloy Sheet	27

<u>ACKNOWLEDGEMENTS</u>	28
--------------------------------	----

1. INTRODUCTION

Shigeru Machida, Japan Aerospace Exploration Agency

This review summarizes the papers on the study of aeronautical fatigue, structural integrity and related themes conducted in Japan during June 2017 to May 2019.

The papers were contributed by following organizations:

Acquisition, Technology & Logistics Agency (ATLA)

Japan Aerospace Exploration Agency (JAXA)

R&D Institute of Metals and Composites for Future Industries (RIMCOF)

Mitsubishi Heavy Industries, Ltd. (MHI)

Mitsubishi Aircraft Corporation

Kawasaki Heavy Industries, Ltd. (KHI)

SUBARU CORPORATION

IHI Corporations

ShinMaywa Industries, Ltd.

Toray Industries, Inc.

The University of Tokyo

Nagaoka University of Technology

Shizuoka University

Tokyo Metropolitan University

Waseda University

Kanagawa Institute of Industrial Science and Technology

The general activities on aircraft development program in Japan during 2017 to 2019 is summarized as follows:

- The development of MRJ (Mitsubishi Regional Jet, 70-to 90-seat regional jets) aircraft is in the final stage and various steps for the certification is being made. The first flight was successfully completed in November 2015. The production is underway at Mitsubishi Aircraft Corporation in Nagoya. In January 2018, high altitude testing was conducted in Arizona in U.S.A. and MRJ performed flight demonstration at Farnborough in July of the same year. Certification flight testing started in January 2019 at Moses Lake in U.S.A.
- Japanese companies are playing an important role in the global joint development of the Trent1000, GENx and other engines for Boeing787 and are taking part as the manufacturer of the low pressure turbine components of GE9X engines for Boeing777X. In March 2018, the engine was tested under the wing of GE Aviation's 747 flying testbed. Also, Japanese companies are participating in global joint development of the PW1100G-JM engine for the Airbus A320neo to achieve fuel-efficiency, low-pollution, and noise-reduction, with P&W taking the lead.
- XP-1 Maritime Patrol Aircraft succeeded in the first flight in September 2007 and started delivering to the base from March 2013. XP-1 as P-1 made demonstration flights at Berlin Airshow in July 2017. XC-2 Transport Aircraft successfully completed its first flight in January 2010 and first delivery to the base as C-2 was in March 2017.
- R&D Institute of Metals and Composites for Future Industries (RIMCOF) was established in July 2016 to promote R&D efficiency in materials and structures development for new aircraft in collaboration with industries, universities and national laboratories. RIMCOF is responsible to operate "Civil Aviation Fundamental Technology Program -Advanced Materials & Process Development for Next-Generation Aircraft Structures" supported by NEDO (New Energy and Industrial Technology Development Agency). The program includes three projects on (1) Practical Use of Structural Health Monitoring (SHM) for Composite Aircraft, (2) High Rate Manufacturing of CFRP Parts, and (3) Material Development and Processing of Next-Generation Magnesium Alloys.
- "Structural Materials for Innovation" (SM⁴I) Project started in 2014 as a part of SIP

(Cross-ministerial Strategic Innovation Promotion Program) supported by the Council for Science, Technology and Innovation (CSTI) of the Cabinet Office, Japan. New material development is underway in the following areas; (1) High Rate Production CFRP Materials, (2) High Temperature Alloys and Intermetallic Compounds, (3) Ceramic Coatings and Ceramic Matrix Composites (CMC), and (4) Materials Integration. The CFRP materials in development covers, OoA (Out-of-autoclave) prepregs, Advanced Resin Transfer Molding (RTM) materials, Advanced Thermoplastic prepregs, High Temperature Polyimide CFRP prepregs. Process and life cycle monitoring technologies are utilized to establish the manufacturing modeling codes for cost effective material certification. The first phase of SIP ended in 2018 being followed by the second phase. From the material development point of view, its purpose is to develop a next-generation Materials Integration (MI) system for the inverse design creating desired performance, materials and process, leading the world utilizing the technical foundation of MI being developed so far. Following three domains construct the research project: A: Establishment of Inverse Design MI Basis for Advanced Structural Materials and Processes, B: Application of the Inverse Design MI to Actual Structural Materials (CFRP), and C: Application of the Inverse Design MI to Actual Structural Materials (3D Powder Processing). The developed material and process plan to use the aircraft structure and the engine.

- The Weather (Weather Endurance Aircraft Technology to Hold, Evade and Recover) -Eye consortium was established in 2016, in order to improve the operational safety and efficiency under the severe weather condition. A slippery short runway in winter, severe lightning, crystal ice drop and volcanic ash were selected for research topic. From the material point of view, development of the CFRP with high conductivity through the thickness direction using conductive polymer have been conducted to reduce the lightning damage. High conductive polymer was developed and the reduction of the lightning damage using the polymer was demonstrated. The modification of the polymer was underway.
- From 5th to 6th of June, ICAF2017 36th conference was held in Nagoya, Japan followed by ICAF2017 29th symposium, from 7th to 9th, which featured some new efforts to promote more participation. Several organized sessions were prepared including Structural Health Monitoring (SHM) and Material Innovation. The total number of participants was more than 200 from 22 nations.

2. FATIGUE AND FAILURE IN METALLIC MATERIALS AND COMPONENTS

2.1 Fatigue Characteristic of Linear Friction Welded Ti-6Al-4V Joints

Hiroshi KUROKI¹, Yukihiro Kondo¹, Tsukasa Wakabayashi¹, Kenji Nakamura¹,
Kikuo Takamatsu¹, Koji Nezaki¹, Mitsuyoshi Tsunori¹
¹*IHI Corporation, Tokyo, Japan*

A blisk is the integrated part of rotating blades and a disk, which is recently being adopted for fan and compressor modules of jet engines for the purpose of the weight reduction and the performance improvement. The blisk is generally manufactured by milling from the large forged material. Therefore large amount of material is wasted as cutting chips. Linear friction welding (LFW) is expected to save the wasted material, which is a kind of the solid state joining. (see Figure 2.1-1) The purpose of this study was to investigate the reduction of the fatigue strength due to LFW process.

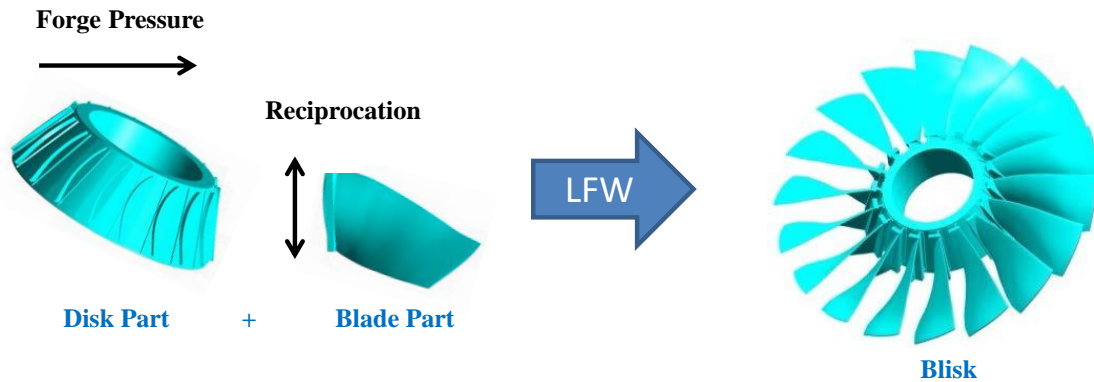


Figure 2.1-1. Schematic View of Blisk Fabrication using LFW

The fatigue test specimens of LFW joints and the base material were made from the same forged material to minimize the effect of scatter. Fatigue tests and analysis of covariance were conducted, and it was made clear that the fatigue strength of as-welded joint was slightly lower than that of base material, and that that of post weld heat treated (PWHTed) LFW joint was the same as that of base material. (see Figure 2.1-2) Since it was thought that the fatigue strength reduction of as-welded LFW joint was due to the effect of residual stress, the residual stress was measured before and after PWHT by Center Hole Drilling method. It was confirmed that the residual stress of as-welded LFW joint remained approximately 3mm from the weld line (see Figure 2.1-3) where the fracture occurred in the fatigue tests, and that the residual stress of PWHTed LFW joint was reduced drastically. As a conclusion, it was made clear that the fatigue strength of PWHTed LFW joint was equivalent to that of base material with the statistical data.

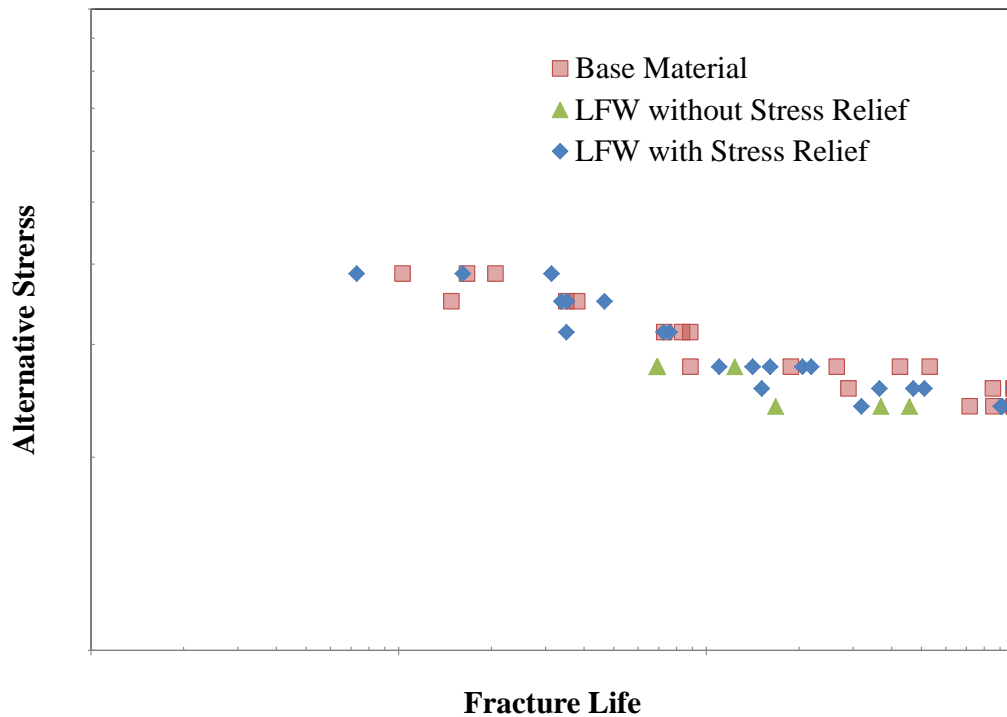


Figure 2.1-2. Results of Fatigue Tests

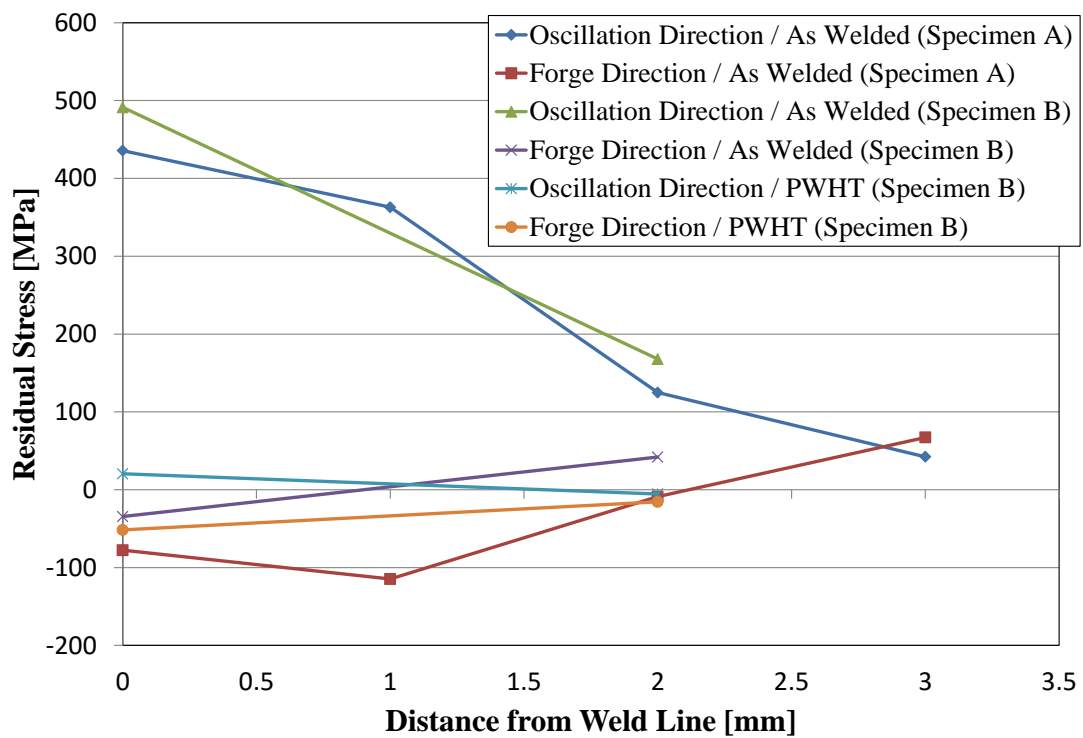


Figure 2.1-3. Result of Residual Stress Measurement

2.2 Interaction between High- and Low-cycle Thermo-mechanical Fatigue Loadings in Small Crack Growth around Cooling Hole in A Ni-based Superalloy.

Masakazu OKAZAKI¹, Yuuki YONAGUNI¹

¹Nagaoka University of Technology, Niigata, Japan

Cooling hole area introduced in gas turbine blades may be one of susceptible areas to fatigue failures, when gas turbine systems are subjected to frequent load change. Here an interaction between high- and low-cycle thermo-mechanical fatigue failure is an key issue to be concerned. In order to get basic understandings on the structural reliability under such a condition, a new testing system has been developed in this work (Figure 2.2-1(a)). By means of the test system the propagation behavior of the small crack nucleated from a simulated cooling hole in a directionally solidified Ni-base superalloy was studied under the artificial condition in which the high-cycle thermo-mechanical fatigue (TMF) loading was superimposed on the stationary low-cycle TMF loading (Figure 2.2-1 (b)). The experimental works demonstrated that the role of the high-cycle thermal stress cycle resulting from non-stationary response of the structure significantly interacted with the stationary low cycle TMF loading (Figure 2.2-2).

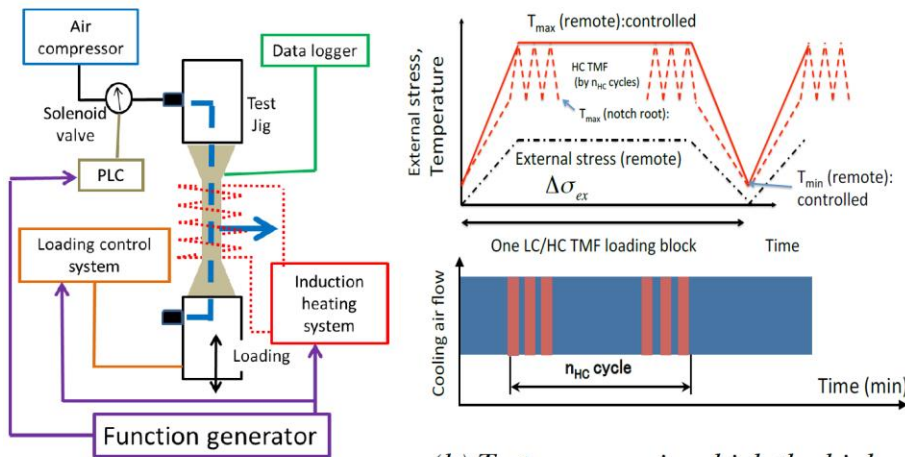


Figure 2.2-1. A new test system developed and the test program performed.

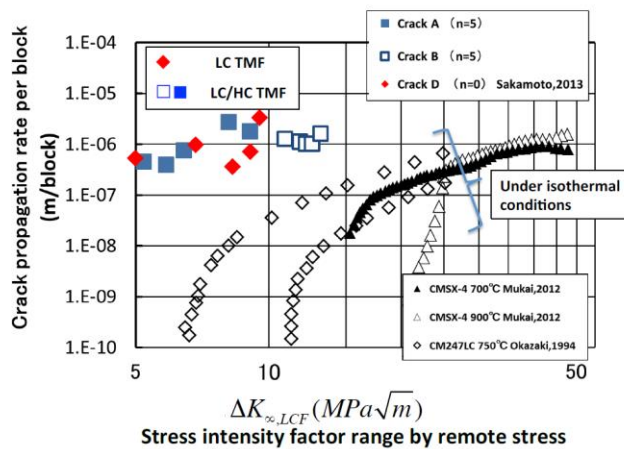


Figure 2.2-2. Low cycle TMF crack propagation rates significantly affected by the superimposed high-cycle thermal fatigue loadings.

2.3 Fatigue Life and Fatigue Crack Growth Behavior of Non-through Cracks in Friction Stir-Welded 2024-T3 Aluminum Alloy

Takao Okada ¹, Shigeru Machida ¹, Naoyuki Watanabe ²

¹*Japan Aerospace Exploration Agency, Tokyo, Japan*

²*Tokyo Metropolitan University, Tokyo, Japan*

Friction stir welding was invented in 1991, and it has been intended to be applied to primary aircraft structures, and then wide range of research have been conducted in order to evaluate its properties, such as elastic, plastic, fatigue, fatigue crack growth and corrosion resistance and so on. Friction stir-welded (FSW) joints were evaluated under two welding conditions to investigate hardness and fatigue property and presented in the ICAF2011 Japanese national review. Here, static and fatigue test were additionally conducted and fatigue crack growth behavior were also evaluated based on the fracture surface observation. Fatigue test of the riveted joint using same skin thickness were also conducted.

Static test, fracture surface observation and hardness evaluation showed that the kissing bond became the fracture origin in welding condition A, while the HAZ which was about 1.2 mm away from the weld center did the fracture origin in welding condition B. The average yield strength of a specimen for welding condition A is 339.4 MPa, 6% higher than that of the base material, and its ultimate strength is 435.2 MPa, 10% lower than that of the base material. The elongation at failure is 8.0% and is 40% of that of the base material. For welding condition B, the average yield strength is 333.4 MPa, 4% higher than that of the base material, and the ultimate strength is 6% lower than that for the base material. The elongation at failure is 12.0% and 60% of that of the base material.

Fatigue test result of the FSW joint and base material in as-received surface conditions were shown in Figure 2.3-1. For welding condition A, the slope of the S-N curve when the kissing bond is the origin of the fracture is indicated by a thick solid line, and the curve when the tool mark near the burr is the origin of the fracture is indicated by a thick dashed line. For welding condition A, a tool mark near a burr can be the origin of a fracture at stresses above the fatigue limit because the stress concentration around it is a source of fatigue failure. On the other hand, the kissing bond is not an origin of fractures at lower stress levels because it does transfer stress at such stress levels. When the kissing bond is the origin of a fracture, the fatigue life of the joint is much shorter than that when a tool mark near the burr is the origin of fracture. The higher fatigue life was obtained for welding condition B comparing to that for welding condition A. Because the size of the tool mark and reduction of thickness for welding condition B were smaller than those for welding condition A, their effects on the origin of the fracture and fatigue life become less detrimental. The fatigue test result of the riveted joints were also shown in Figure 2.3-1. A countersunk rivet made of a 2117-T4 aluminum alloy was used to fasten the joint. The single lap joint specimen was manufactured by three rows of three fasteners. Its fatigue life was much lower than that for FSW joint. Figure 2.3-2 showed the relationship between the fatigue life and the ratio of stress range to the tensile stress of the joint, because the tensile stress of the joint were different from the type of the joint. The fatigue life was run-out for FSW joint where the stress range/tensile strength was below 0.3, while the riveted joint fractured less than a million cycles.

Fatigue crack growth behavior based on the fracture surface observation were shown in Figure 2.3-3. The stress intensity factor range for welding condition A was obtained for the edge crack with equal crack length along the width direction of the specimen. On the other hand, the stress intensity factor for the corner crack in welding condition B was calculated using the equations proposed by Newman et al. The crack growth rate when a kissing bond is the origin of the fracture is close to that of the base material obtained from the middle tension specimen. The crack growth rate when a tool mark near a burr is the origin of the fracture is different from that of the base material; overestimating the stress intensity factor range based on assuming the crack geometry contributes to the difference. The crack growth rates for welding condition B relatively coincides with that of the base material.

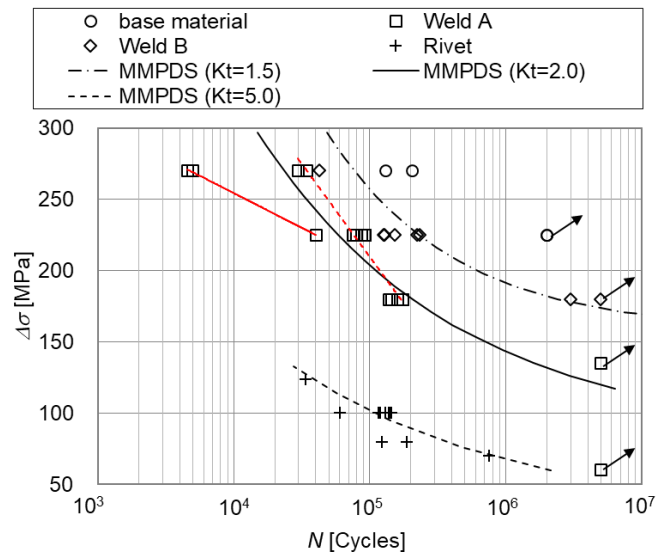


Figure 2.3-1. Fatigue test results for FSW and rivete joint.

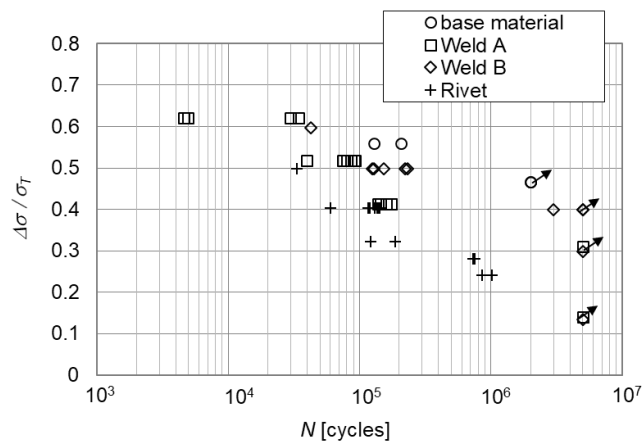


Figure 2.3-2. Relationship between stress range/tensile strength and fatigue life.

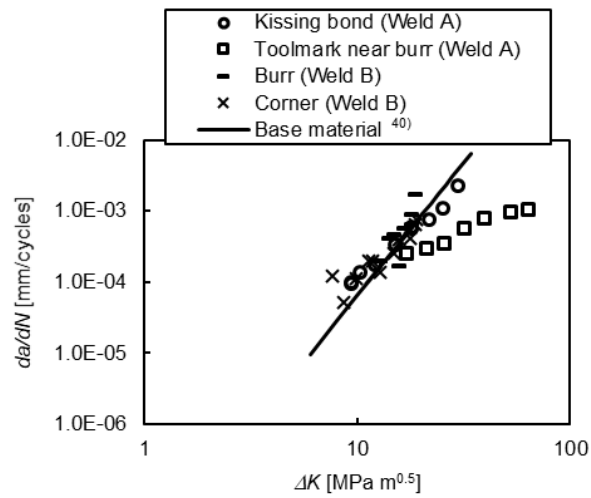


Figure 2.3-3. Fatigue crack growth rate of the FSW specimen.

3. FATIGUE AND FAILURE IN COMPOSITE MATERIALS AND COMPONENTS

3.1 Ply Curving Termination to Suppress Delamination in Composite Ply Drop-Off

Shu Minakuchi¹, Nobuo Takeda¹
¹The University of Tokyo, Chiba, Japan

In a lightweight aircraft composite structure, it is desirable to decrease the plate thickness in low-load areas by terminating unnecessary plies (i.e., ply drop-off). It is possible to significantly save the structural weight by steeply changing the thickness in response to the local load distribution. However, tapered sections with steep taper angles act as initiation points of delamination. It is known that stress concentrates at the edge of the terminated 0° plies that have the fiber direction in parallel to the loading direction. As a result, current aircraft composite structures use quite gradual taper angles and have unnecessary thick parts in the low-load areas. Structural modification that can suppress the stress concentration at the edge of the terminated 0° plies is necessary to realize further-optimized lightweight structures with steeper taper angles.

This study proposes a new approach called “ply curving termination (PCT)” that locally changes the fiber orientation at the edge of the termination 0° plies. Figure 3.1-1 shows the most basic form of ply drop-off where one 0° ply is laminated on the base laminate. In the conventional part in Figure 3.1-1 (a), in-plane tensile loading induces stress concentration at the edge of the terminated 0° ply and secondary bending due to the eccentric load path along the ply drop-off, which leads to delamination initiation. In contrast, the PCT structure in Figure 3.1-1 (b) has the curved edge that has significantly low stiffness in the loading direction (e.g., when the curved angle is 45° with standard carbon/epoxy, the elastic modulus decreases to about 10%). This modification suppresses the stress concentration and secondary bending at the edge of the terminated ply, so stress is gradually transferred from the base laminate to the terminated ply. In addition, even if delamination occurs from the edge, its propagation is suppressed in the curved area because the stiffness of the delaminated edge is low. Meanwhile, the terminated ply far away from the edge can fulfill the original purpose of strengthening the base laminate because the fiber direction is along the loading direction.

This study validated the effectiveness of the proposed concept through numerical analysis and experiments. Finite element analysis was first conducted (Figure. 3.1-2). It was confirmed that secondary bending due to the eccentric load path along the ply drop-off is suppressed by PCT (45° specimen), and the out-of-plane stress at the edge of the terminated ply is significantly reduced. Validation tests were then performed under static and fatigue loading conditions (Figure. 3.1-3). It was successfully demonstrated that the proposed structure significantly delays delamination initiation and propagation.

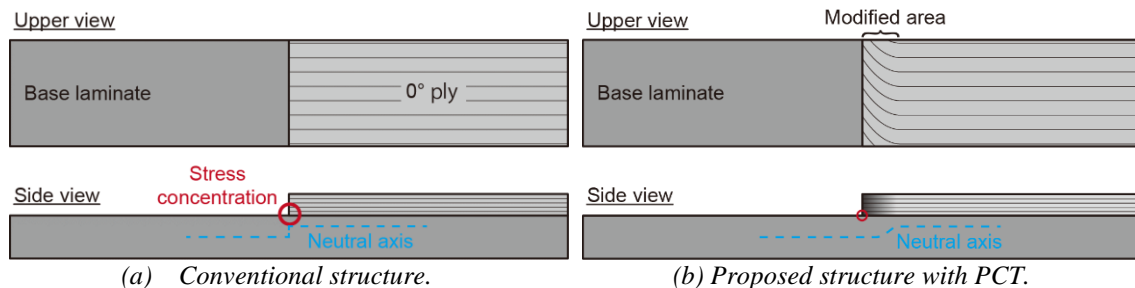


Figure 3.1-1. Stress concentration at edge of terminated 0° ply.

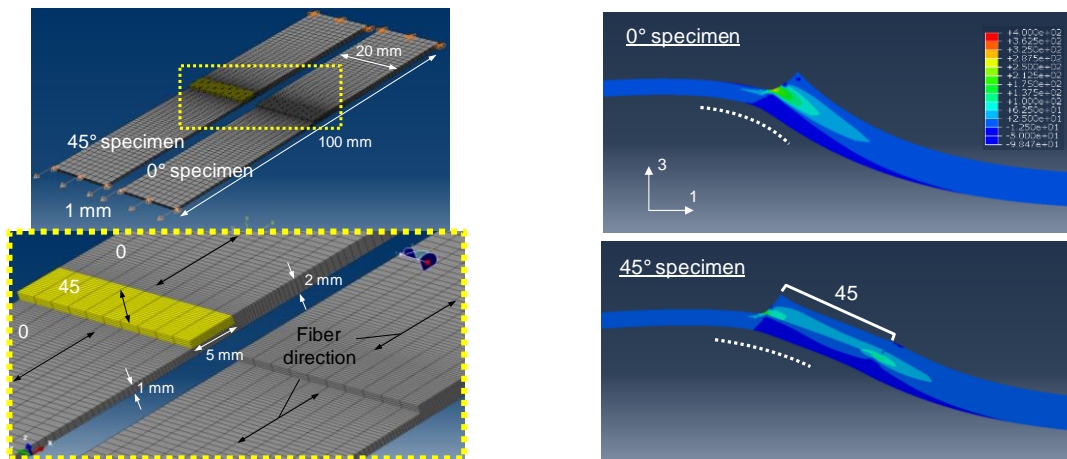


Figure 3.1-2. Finite element analysis.
 (Left) Finite element models. 45° specimen includes PCT.
 (Right) Deformation and out-of-plane shear stress τ_{13} at edge of terminated ply. Displacement magnification factor is 20.

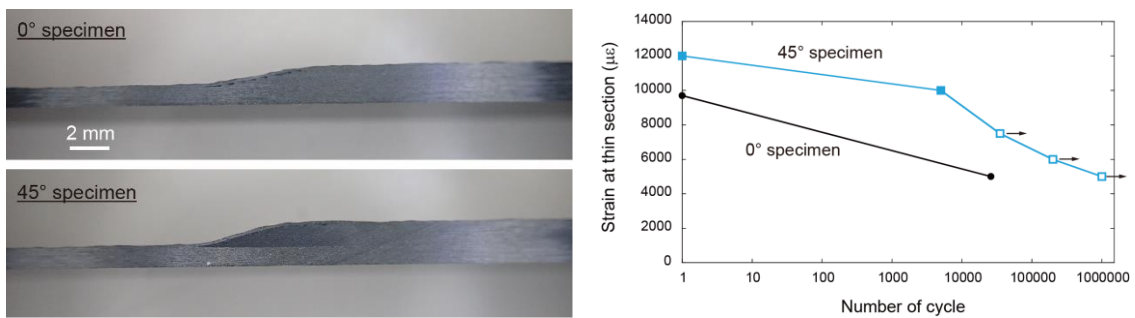


Figure 3.1-3. Validation test results using specimens with taper ratio of 1:5.
 (Left) Cross-section of tapered specimens. Fiber direction of base laminate and terminated plies were 0°. 45° specimen had 5 mm long PCT section at edge of terminated plies.
 (Right) Static and fatigue test results. White markers indicate that specimens did not fail.

3.2 Very High-Cycle Fatigue Characteristics of Cross-Ply CFRP Laminates in Transverse Crack Initiation

Atsushi Hosoi¹, Takuro Suzuki¹, Kensuke Kosugi¹, Takeru Atsumi¹,
Yoshinobu Shimamura², Terumasa Tsuda³, Hiroyuki Kawada¹

¹Waseda University, Tokyo, Japan

²Shizuoka University, Shizuoka, Japan

³Toray Industries, Inc., Ehime, Japan

Carbon fiber reinforced plastic (CFRP) laminates are lightweight and have excellent mechanical properties. Thus, they have been used not only for aircraft fuselages and wings but also for engine parts. Especially, fan blades are subjected to very high cyclic loadings during the design life, so it is essential to evaluate the giga-cycle fatigue characteristics of CFRP laminates. In this study, the transverse crack initiation of the cross-ply CFRP laminates in very high-cycle fatigue region was evaluated using an ultrasonic fatigue testing machine. The cross-ply $[0/90_4]_s$ CFRP laminates were formed from interlaminar toughened type prepreg, T800S/3900-2B, with fiber volume fraction of $V_f = 56\%$ and cured at 453 K in an autoclave. The fatigue tests were conducted at the frequency of $f = 20$ kHz and the stress ratio of $R = -1$. In order to suppress temperature rise of the specimen, the intermittent operation with the loading time of 200 msec and the pausing time of 2000 msec was adopted. The fatigue life data to transverse crack initiation in very high-cycle fatigue region was compared with the data of the fatigue test which was conducted at the frequency of $f = 5$ Hz and the stress ratio of $R = 0.1$ using a hydraulic control fatigue test machine. Figure 3.2-1 shows the transverse crack observed on the specimen edge surface at the $N = 4.3 \times 10^8$ cycles and under the test condition of initial maximum strain of $\epsilon_{\max} = 0.15\%$. The transverse crack passed through the thickness and width directions of the specimen perpendicular to the loading axis. Figure 3.2-2 shows the fatigue life diagram to the transverse crack initiation. It was evaluated considering the influences of the stress ratio and the thermal residual stress by using the modified Walker model [1]. The vertical axis of the graph was expressed with the product of the normalized maximum stress and stress amplitude applied in 90° layers of the cross-ply laminates. From this results, the fatigue life to the transverse crack initiation of the cross-ply CFRP laminates in the very high-cycle region exceeding 10^8 cycles was on the extension of the test data in the low cycle region.



Figure 3.2-1. Transverse crack observed on the specimen edge surface.
($\epsilon_{\max} = 0.15\%$, $N = 4.3 \times 10^8$ cycles)

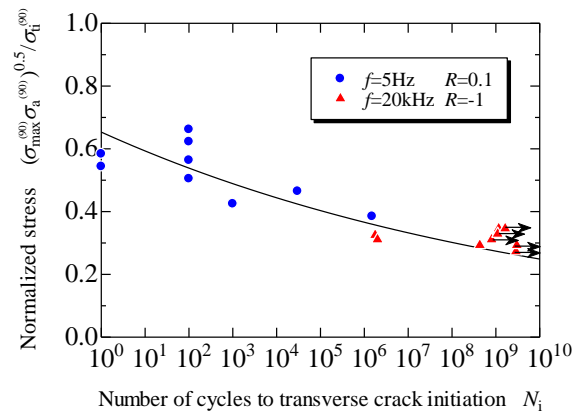


Figure 3.2-2. Fatigue life diagram to transverse crack initiation.

References

[1] Atsushi Hosoi, Hiroyuki Kawada, Fatigue life prediction for transverse crack initiation of CFRP cross-ply and quasi-isotropic laminates, *Materials*, 2018, 11(7), 1182.

3.3 Damage mechanisms and mechanical properties of directly bonded CFRTP and aluminium with nano-structured surface

Kristine Munk Jespersen^{1,2}, Hikaru Abe², Hiroki Ota², Kei Saito², Keita Wada², Atsushi Hosoi², Hiroyuki Kawada^{2,3}

¹Kanagawa Institute of Industrial Science and Technology (KISTEC), Kanagawa, Japan

²Waseda University, Tokyo, Japan

³Kagami Memorial Research Institute for Material Science and Technology, Waseda University, Tokyo, Japan

In recent years, the aerospace and automobile industries are increasingly focusing on decreasing the weight of the structures to improve the fuel efficiency and thereby reduce the global CO₂ emissions. As a result, lightweight, stiff and strong carbon fibre reinforced plastics are increasingly replacing metals in the design. Particularly, carbon reinforced thermoplastics (CFRTPs) are of recent interest due to their high impact performance along with their great formability and possibility for recycling. In addition, initiatives for moving away from heavy mechanical joints such as “a fully bonded aircraft” are arising. However, it is rarely feasible to replace an entire structure with CFRTPs, and thus dissimilar material bonding, will be necessary to achieve such goals. However, adhesively joining CFRTP to commonly used metals such as aluminium generally results in low bonding strength, and thus alternative bonding methods are of interest. Thus, the current study investigates the mechanical properties and damage mechanisms of a recently proposed method to directly bond CFRTP and aluminium by altering the aluminium surface. This is achieved by a combination of anodizing and etching treatments followed by a silane coupling treatment, resulting in a nano-structure on the aluminium surface (e.g. Figure. 3.3-1). After the treatment, the CFRTP and aluminium are bonded by hot-pressing. High static bonding strength is confirmed by single-lap tensile tests. In addition, double cantilever beam (DCB) and end notched flexure (ENF) are carried out both under static and fatigue loading, where the nano-structure is observed to significantly improve the strength and fatigue lifetime of the bonded joint. In order to investigate the interface properties and damage mechanisms in more detail, the tests are monitored by a digital image correlation (DIC). DIC is used to track the local deformation of the specimen edge by applying a random pattern paint, making it possible to measure the local crack opening and shear displacements. Figure. 3.3-2 shows an example of the crack and points tracked by DIC. This allows for the determination of the cohesive law, which can be directly used in finite element simulations.

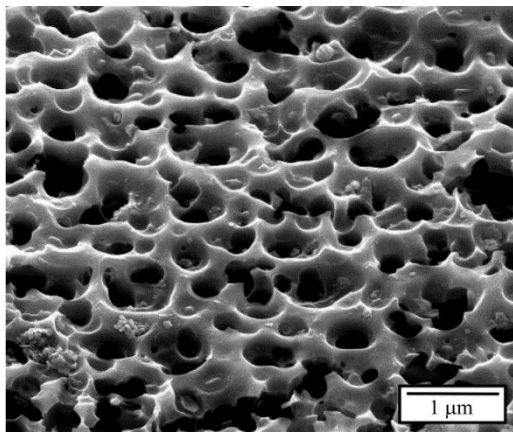


Figure 3.3-1. Example of one type of nano-structure manufactured on the aluminium surface.

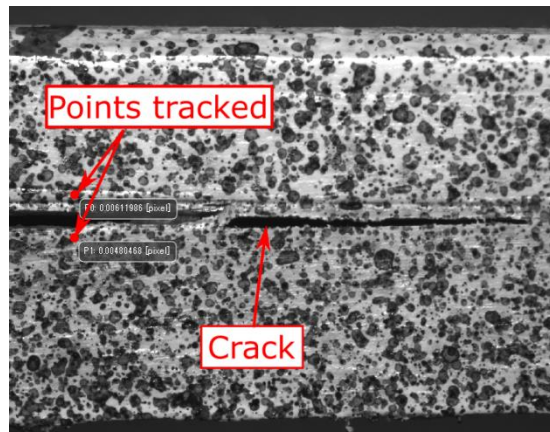


Figure 3.3-2. Example of the DCB specimen during crack growth with random pattern paint

3.4 Tensile Test of Ti/CFRP Scarf Joint with One Stringer

Hikaru Hoshi¹, Sunao Sugimoto¹, Yutaka Iwahori¹, Toshiya Nakamura¹
¹Japan Aerospace Exploration Agency, Tokyo, Japan

JAXA aims to reduce weight of single aisle aircraft by usage of composite material and widely use of adhesive joint. In this study, we have a plan to apply adhesively scarf joint to the wing-body joint structure, and we are considering adopting of the CFRP/Ti6Al4V scarf joint.

A tensile test was conducted to confirm the load capability of the Ti/CFRP scarf joint which simulated wing cover root joint. The test article was endured the ultimate load condition without significant damage at joint region. After that, we estimated simply how much weight can be reduced by adhesive joint compared with the conventional bolted joints. As a result of estimation, it is thought that adhesive joint able to reduce 28% against the weight of the conventional bolted joint.

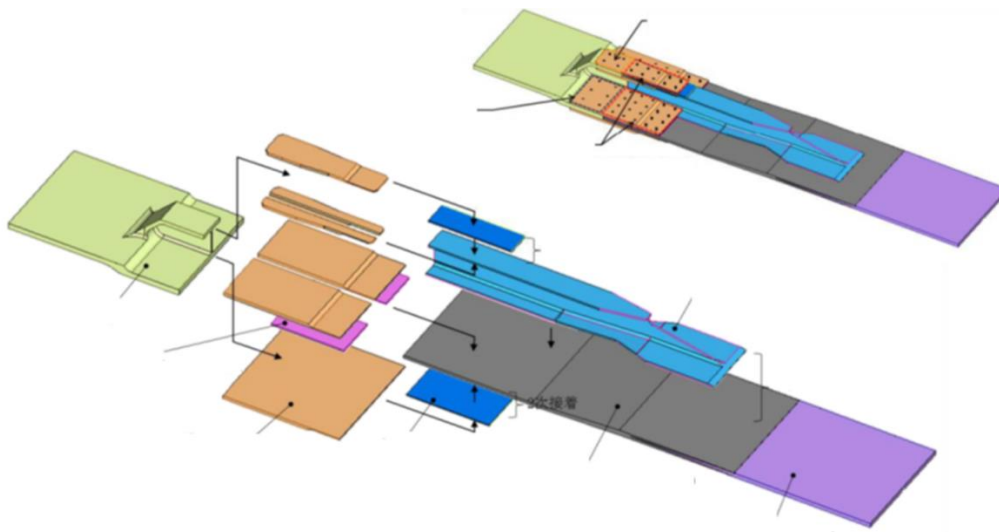


Figure 3.4-1. Test article of Ti/CFRP Scarf Joint with One Stringer

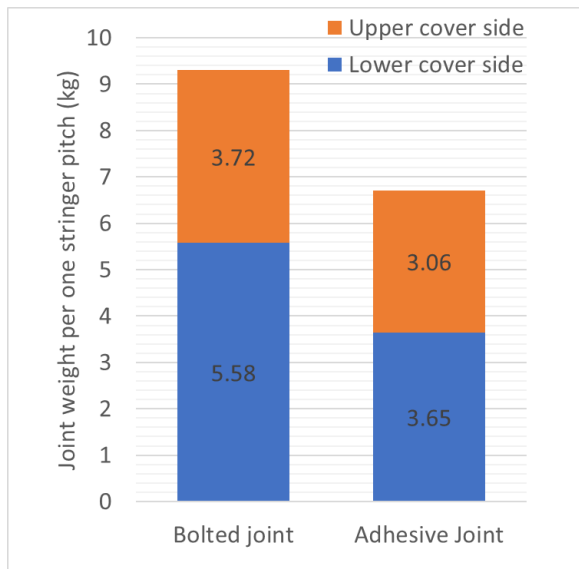


Figure 3.4-2. Wing cover root joint weight comparison between bolted joint and adhesive joint.

4. STRUCTURAL HEALTH MONITORING

4.1 Flight testing of an ultrasonic based SHM system

Hideki Soejima¹, Takuya Nakano¹, Makoto Yokozuka¹, Yoji Okabe², Nobuo Takeda^{3,4}, Noriyuki Sawai³

¹ SUBARU CORPORATION, Tochigi Japan

² The University of Tokyo, Tokyo Japan

³ R&D Institute of Metals and Composites for Future Industries, Tokyo Japan

⁴ Japan Aerospace Exploration Agency, Tokyo Japan

We have been developing an Ultrasonic based structural health monitoring (SHM) system which can provide essential information on structural integrity of airframes. The SHM system can be used in whole aircraft lifecycle from design phase to disposal / recycle phase. In order to achieve implementation of the SHM system, we have conducted various types of tests, in which we assessed damage detection capability, accuracy and probability of damage detection, environmental durability, and applicability to aircraft system, and so on, based on the building block approach. In the SHM system, ultrasonic waves are generated and measured with micro actuators and optical fiber sensors which are installed in aircraft structures directly. When damages initiate and grow in the structures, ultrasonic waves which propagate through the structures are influenced and changed by the damages. The changes of the ultrasonic waves are analyzed in the SHM system; consequently, the damages can be detected. Overview of the SHM system is shown in Figure 4.1-1.

In order to evaluate compatibility to an actual aircraft and detection capability in actual aircraft operating conditions, which influence to measurement of ultrasonic waves, flight testing for the SHM system was conducted. Micro actuators and optical fiber sensors were installed to airframes directly and to a test specimen which was installed to an airframe as well. An interrogation unit and control PC were also installed in the cabin with a rack. The flight testing was conducted with a flying test bed (FTB), which was modified by Japan aerospace exploration agency (JAXA) from a biz-jet class aircraft, Sitation Sovereign, manufactured by Cessna. Some flight maneuvers were carried out in a series of the flight testing and ultrasonic waves were measured not only on ground but also in-flight conditions. From the result of the flight testing, it was confirmed that ultrasonic waves could be measured in-flight conditions just like those measured on ground and damages introduced to the test specimen could be detected by analyzing the changes in waveforms of the ultrasonic waves even in the actual operating aircraft.

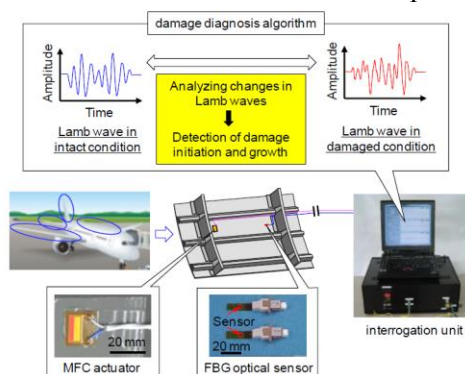


Figure 4.1-1. Overview of the ultrasonic based SHM system.

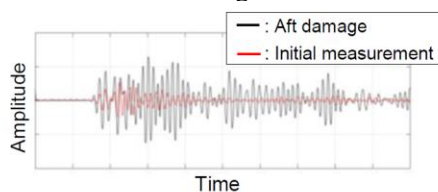


Figure 4.1-2. ultrasonic waves before and after damage measured in the test specimen.

4.2 Real-time Stress Concentration Monitoring of Aircraft Structure during Flights using Optical Fiber Distributed Sensor with High Spatial Resolution

Daichi Wada¹, Hirotaka Igawa¹, Masato Tamayama¹, Tokio Kasai¹, Hitoshi Arizono¹, Hideaki Murayama²

¹*Japan Aerospace Exploration Agency, Tokyo, Japan*

²*The University of Tokyo, Chiba, Japan*

For efficient and reliable design and operation of aircraft, monitoring of deformation and strain during flights is beneficial. Optical fiber sensors are highly applicable for this purpose. They are light-weighted and flexible, which allows less invasive installation to aircraft structures. In addition, they are capable of distributed monitoring, which enables efficient measurements by collecting strain distributions along a single fiber. By using optical fiber distributed sensors with a high spatial resolution such as mm order, it is even possible to monitor local strain distribution profiles at stress concentration areas. The stress concentration is critical for structural integrity, whereas difficult phenomenon to predict and accurately observe without such a distributed sensing technique.

We have developed an optical fiber distributed sensing technique using long-length fiber Bragg gratings (FBGs) and optical frequency domain reflectometry (OFDR). The OFDR-FBG technique allows us to monitor real-time strain distributions during flights along the FBGs with a 1.6 mm spatial resolution and a 151 Hz sampling rate [1, 2]. We applied this monitoring technique to a middle-sized business jet (Cessna Citation Sovereign), and conducted flight tests. In this study, we report time histories of strain distribution profiles during various maneuvers especially focusing on stress concentration areas.

Figure 4.2-1 shows the sensing configuration for the flight tests. We conducted two campaigns of the flight tests. For the first campaign (in 2016), we monitored a stringer of the fuselage and the aft-bulkhead. We bonded a 5 m-long FBG along the stringer and a 50 cm-long FBG to the surface of the aft-bulkhead diametrically. For the second campaign (in 2017), we monitored a main wing. We bonded a 10 m-long FBG to the bottom surface of the wing along the spar.

Figure 4.2-2-4 show examples of monitoring results. Strain values are the variations from the state at which the aircraft was on the ground. Figure 4.2-2 shows a strain distribution along the main wing when the aircraft banked-turned. The position indicated the location from the wing root (= 0 m) to the wing tip (= 8 m). The deflection of the wing with the upward wing tip induced a tensile strain distribution on the bottom side, having larger amplitudes at the root. We added the rib locations with dotted lines in the graph. As clearly seen especially at the wing root, the abrupt strain distribution variations due to the stress concentration existed at the rib locations. Some of them showed larger values, which illustrated the importance of the actual data monitoring. Figure 4.2-3 shows a strain distribution along the fuselage stringer when the aircraft banked-turned. The position indicated the location from close to the main wing (= 0 m) and in the traveling direction. We observed tensile strains having larger values for locations closer to the main wing. At the banked-turn, the fuselage was under bending load, and deflected downwards at the aircraft nose. Therefore, the tensile strains were induced on the top side of the fuselage. We added the locations of the fuselage frames with dotted lines. We saw the agreement between the locations of the frames and the stress concentrations with lower strain amplitudes. This was considered to reflect the stiffening effect. Figure 4 shows a strain distribution of the aft-bulkhead after takeoff. We saw tensile strains, which represented that the bulkhead “inflated” due the lower air pressure outside of the fuselage. On the back side of the aft-bulkhead, there were stiffeners. Among the monitoring area, a part of the stiffener was located at 200 mm. We saw larger tensile strains at the stiffened area. We surmised that the overall deformation of the fuselage due to the air pressure and temperature variations induced bending to the aft-bulkhead, which caused tensile strains at the thicker area with the stiffener.

We could successfully observe overall strain distributions and local stress concentrations, which were insightful. Some of them were the data that was difficult to predict purely by theoretical analysis. This highlighted the importance and the effectiveness of the sensing technique with the high spatial resolution. We will further examine the monitoring data through comparison with structural analysis of the aircraft.

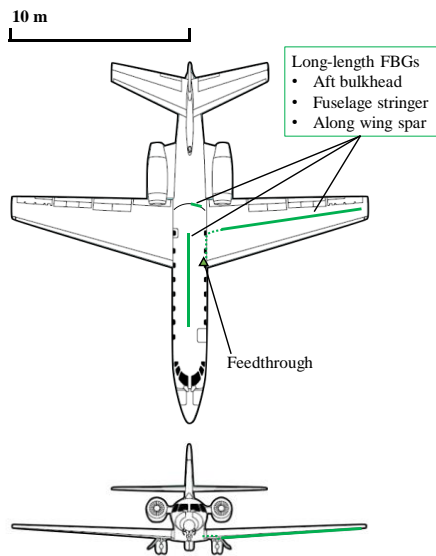


Figure 4.2-1. Sensing configurations for flight tests..

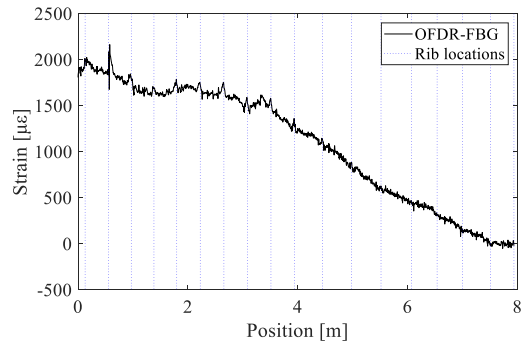


Figure 4.2-2. Strain distribution of main wing during banked turn..

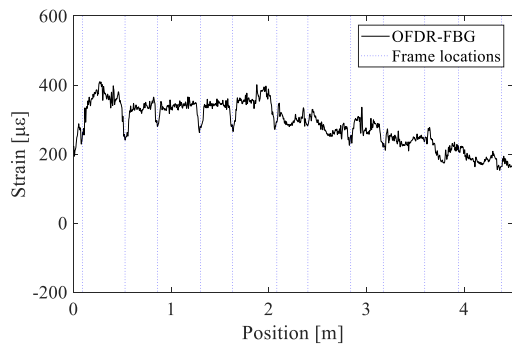


Figure 4.2-3. Strain distribution of fuselage stringer during banked turn..

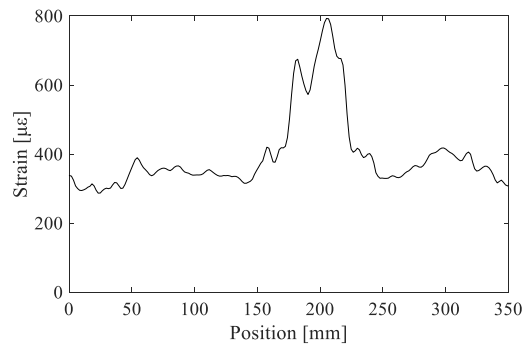


Figure 4.2-4. Strain distribution of aft-bulkhead after takeoff.

References

[1] D. Wada, H. Igawa, M. Tamayama, T. Kasai, H. Arizono, H. Murayama, and K. Shiotsubo, "Flight demonstration of aircraft fuselage and bulkhead monitoring using optical fiber distributed sensing system," *Smart Materials and Structures* 27(2018).

[2] D. Wada, H. Igawa, M. Tamayama, T. Kasai, H. Arizono, and H. Murayama, "Flight demonstration of aircraft wing monitoring using optical fiber distributed sensing system," *Smart Materials and Structures* (2018) (accepted).

4.3 Optical Fiber Sensor based Impact Detection System for Aircraft Structures

Noriyoshi Hirano¹, Keisuke Saito¹, Toru Itoh¹, Toshizo Wakayama¹,
Nobuo Takeda², Noriyuki Sawai², Shu Minakuchi³

¹ *Kawasaki Heavy Industries, Ltd., Gifu, Japan*

² *R&D Institute of Metals and Composites for Future Industries (RIMCOF), Tokyo, Japan*

³ *The University of Tokyo, Chiba, Japan*

The application of composite materials to primary aircraft structure is contributing to the structural weight reduction while composite structures are more susceptible to impact damages that can only be detected through detailed non-destructive inspection (NDI).

Kawasaki Heavy Industries, Ltd. (KHI) has developed a structural health monitoring (SHM) system capable of detecting impact damages using the optical fiber sensors namely Fiber Bragg Grating (FBG) sensors. FBG sensors are ideal for constructing a light-weight sensor network over a wide area of aircraft structures. The SHM system setup is shown in Figure 4.3-1. The FBG measurement unit is airworthy interrogator with 100 kHz sampling rate. The objective of this development is to predict the best maintenance timing to minimize unexpected delays and lost opportunities of aircraft operations due to impact damage.

KHI demonstrated impact detection tests utilized four different impactor materials, namely steel, ice, concrete and rubber. Figure 4.3-2 shows the test setup and the impactors. All these objects created sufficient impact responses for the SHM system to detect the impact. The impact detection method of measuring strains with FBG sensors was established and verified for the aforementioned impact objects.

KHI also performed blunt object impact (BOI) detection test for fuselage skin panel as shown in Figure 4.3-3. BOI damage should be cared for composite fuselage structure because the event is prone to be a catastrophic damage for composite structures with little or no external indication.

Other application demonstrated by KHI was life cycle monitoring with embedded small diameter optical fiber sensor network. The network can monitor the composite part during the fabrication phase, as well as the operation phase.

This work was conducted as a part of the project, "Advanced Materials & Process Development for Next-Generation Aircraft Structures" under the contract from the New Energy and Industrial Technology Development Organization (NEDO), founded by the Ministry of Economy, Trade and Industry (METI) of Japan.

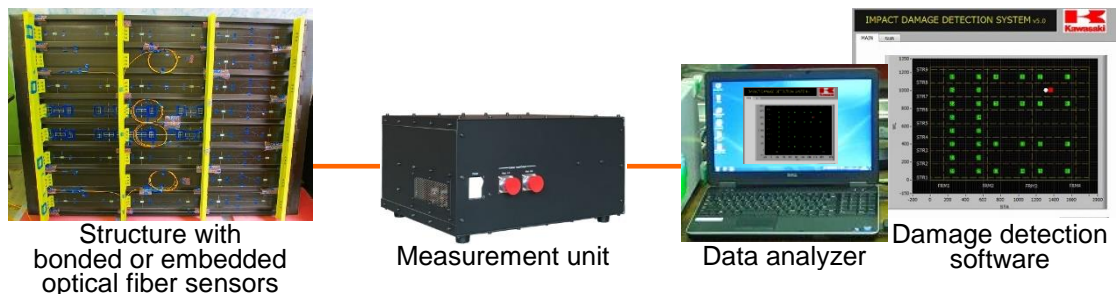


Figure 4.3-1. Impact Damage Detection system

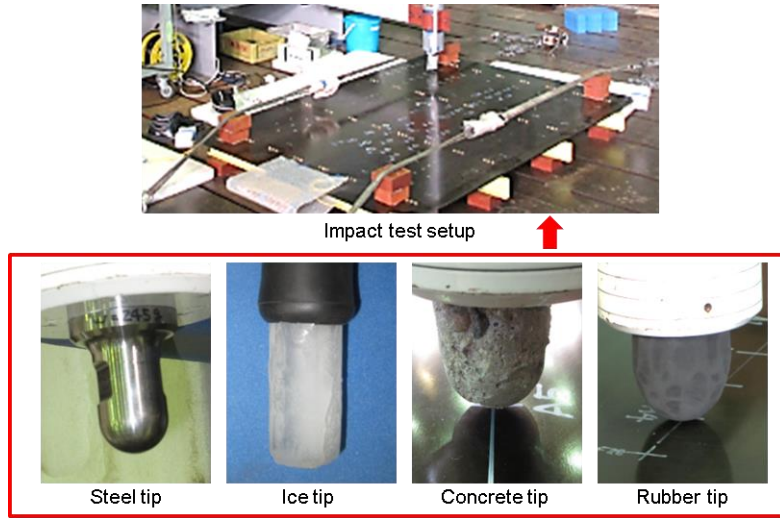


Figure 4.3-2. Impact detection tests using impactors made of various materials

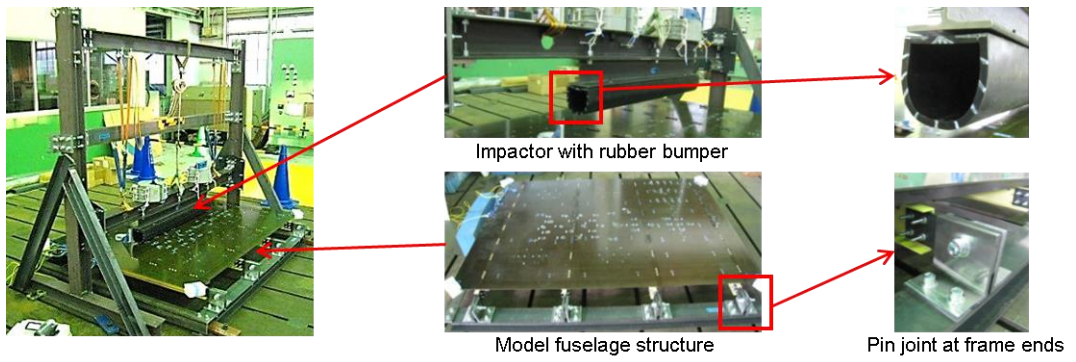


Figure 4.3-3. Blunt object impact tests configuration

4.4 Reconstruction of Local Stress Field using Strain Monitoring Data

Toshiya Nakamura¹

¹*Japan Aerospace Exploration Agency, Tokyo, Japan*

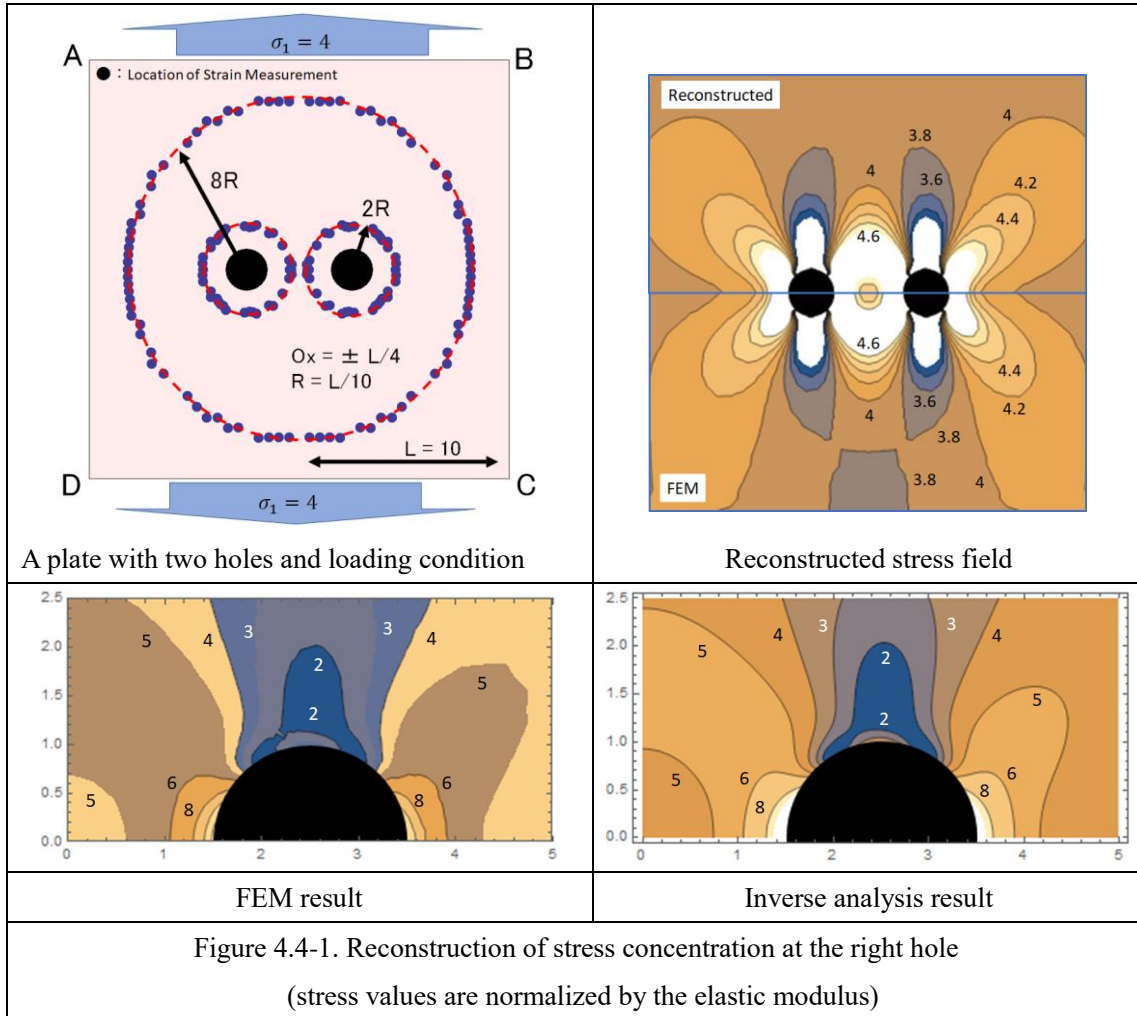
Structural health monitoring includes two concepts. One is the monitoring of strains from which operational loads and/or operational stresses are identified. Another is the detection of structural damage (e.g., cracks and delamination). The former concept can be used to improve the structural design and the optimization of maintenance schedules, based on actual loads or stresses.

The operational stress distribution or the actual stress concentration data can provide an important index for structural fatigue. This is quite useful not only in optimizing the maintenance schedule but also when improving structural design for new aircraft. These are the representative outcomes of the structural health monitoring. It is possible to calculate the stress concentration if both the operational load and the structural model are established. However, there are difficulties with identifying operational loads from strain monitoring data by inverse analysis. Another difficulty is the modeling of the corresponding structure for inverse analysis. Because we encounter a restriction in the area of strain measurement, we cannot obtain the comprehensive strain distribution of the entire structure. Thus, it is inevitable that we focus on the localized area where stress concentration takes place. To do this, however, a question arises about the definition of the boundary of the focused area.

The present study proposes a method to reconstruct the stress distribution and the stress concentration from strain monitoring data. The local area around the strain sensor is scrutinized. The method uses only the strain data obtained inside the area of consideration but does not use the outer boundary conditions (e.g., operational loads). Thus, we expect that the present method will provide an easy method of revealing the actual stress concentration around the hot spot where the fatigue should be assessed.

The method is based on the complex stress functions for plane elasticity problems. The advantage of employing stress functions is that the fundamental conditions of elasticity (i.e., stress equilibrium and strain compatibility) are automatically satisfied.

Example



5. FULL SCALE TESTING

5.1 Full Scale Fatigue Testing for Mitsubishi Regional Jet

Koji Setta¹, Toshiyasu Fukuoka¹, Kasumi Nagao¹, Keisuke Kumagai¹

¹*Mitsubishi Aircraft Corporation*

Mitsubishi Aircraft Corporation is performing the full-scale fatigue testing (FSFT) for Mitsubishi Regional Jet (MRJ) type certification (Figure 5.1-1). Main objective of this test is to show freedom from wide spread fatigue damage (WFD) during the life of aircraft and establish Limit of Validity (LOV). Prior to the test, WFD susceptible structures are defined based on the stress distributions and structure configurations, and they are fully covered by this test. Test duration of FSFT is 240,000 flights (3 x DSG of 80,000 flights). The flight-by-flight loading spectrum (Figure 5.1-2) is newly designed for MRJ and its loads occurrence data was verified by flight test data. Furthermore, to reduce the test duration, low loads omission was applied based on the results of some spectrum verification tests (Figure 5.1-3). During fatigue test, scheduled inspection consistent with MRJ maintenance program is planned. In addition to external and internal visual inspections, some kinds of NDT are applied to the specific area.

Consideration of the specific loads other than major operational loads other than flight, ground, pressurization and control loads is important. For example, thermal stress generated at the hybrid structural joint of composite and metallic structure due to the difference of CTE (Coefficient of Thermal Expansion) may affect fatigue characteristics of airframe. It is not feasible to demonstrate it during FSFT, therefore separated component testing was conducted to validate thermal stress analysis methodology. Full scale composite horizontal stabilizer was installed in the environmental chamber and strain behaviour during thermal cycle was investigated. Through this process, thermal stress spectrum generation process was established.

Since the main objective of FSFT is no WFD substantiation, no artificial crack is introduced during FSFT. Therefore, damage tolerance evaluation (i.e. crack growth analysis validation) is separately conducted by sub-component level testing. For example, damage tolerance substantiation for fuselage structure was performed by using curved panel test facility [1]. This facility can simulate the pressurization load with axial load and their loading sequence can be customized for each test. Major detail design points of fuselage structure such as the lap/butt-joint, cut-out structure and repaired structure are individually evaluated by this type of tests [2]. Based on the test results, potential fatigue critical locations and crack growth behaviors are efficiently investigated, and they significantly contribute to the crack growth analysis validation necessary for CFR/CS 25.571 compliance.

References

- [1] Tsukigase, K., Fukuoka, T., Kumagai, K., Nakamura, T., Taba, S. In: Curved Panel Fatigue Test for MRJ-200 Pressurized Cabin Structure, Proceedings of the 28th ICAF Symposium, Helsinki, 3–5 June 2015, pp. 276–286.
- [2] Setta, K., Fukuoka, T., Kumagai, K., Nakamura, T., Taba, S. In: Structural Damage and Repair Assessment for MRJ Aircraft, Proceedings of the 29th ICAF Symposium, Nagoya, 7–9 June 2017, pp. 1286–1292.



Figure 5.1-1. MRJ90 full scale fatigue test setup

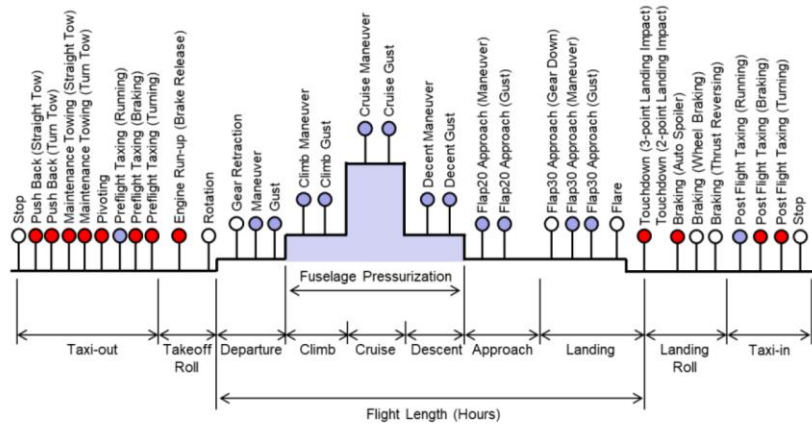


Figure 5.1-2. Flight profile considered in spectrum loading

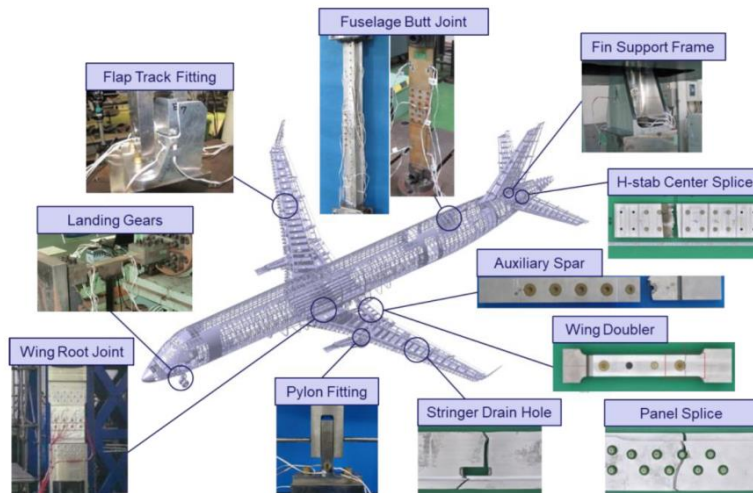


Figure 5.1-3. S-N curve investigations and test spectrum verifications

5.2 Research on Lightweight Airframe Structure

Yasuhiro Kanno¹, Daishi Hijikuro¹, Keisuke Umezawa¹ and Toshimitsu Hayashi¹

¹ *Acquisition Technology and Logistics Agency (ATLA), Tokyo, Japan*

The research on lightweight airframe structure is being carried out to reduce structural weight of future fighters, since stealth capability, including internal weapon bays, tends to increase the structural weight of fuselage significantly. In order to reduce the weight of the fuselage we're focusing on three features, the integrated bonded structure, the heat shield and the efficient and accurate structural analysis techniques.

The integrated bonded structure is made of CFRP (Carbon Fiber Reinforced Plastics) parts with secondary bonding process. Bonding of CFRP parts can reduce the structural weight by reducing the number of fasteners and decreasing CFRP's thickness which has been needed for fastener joints. Bonded structures also make the fuselage parts simpler than conventional ones, which can also reduce the weight.

The aft-fuselage experiences too much high temperature to apply light materials, which has prevented to decrease the weight of the aft-fuselage. The heat shield is a cover surrounding a jet-engine which can shield heat from the jet-engine and allow the use of lighter materials to outer parts of the heat shield.

The efficient and accurate structural analysis techniques establish rules for FEM (Finite Element Method) modeling, automatically convert CAD data to the detailed FEM models and obtain criteria to evaluate integrity directly from the FEM estimation. Using the detailed FEM models, both weight reduction and risk reduction will be anticipated.

This project has three phases. In phase 1, the sub-component of the mid-fuselage was fabricated and tested to validate the bonding technology and the analytical estimation. The results of phase 1 was used in the design of phase 2 full scale mid-fuselage including a part of the aft-fuselage. The strength tests of the fuselage are being conducted and will end in 2019. In the last phase, the fatigue tests of bonded structures under severe environments are planned. After coupon specimens are tested, the specimens cut out from newly-made full scale mid-fuselage will be tested.

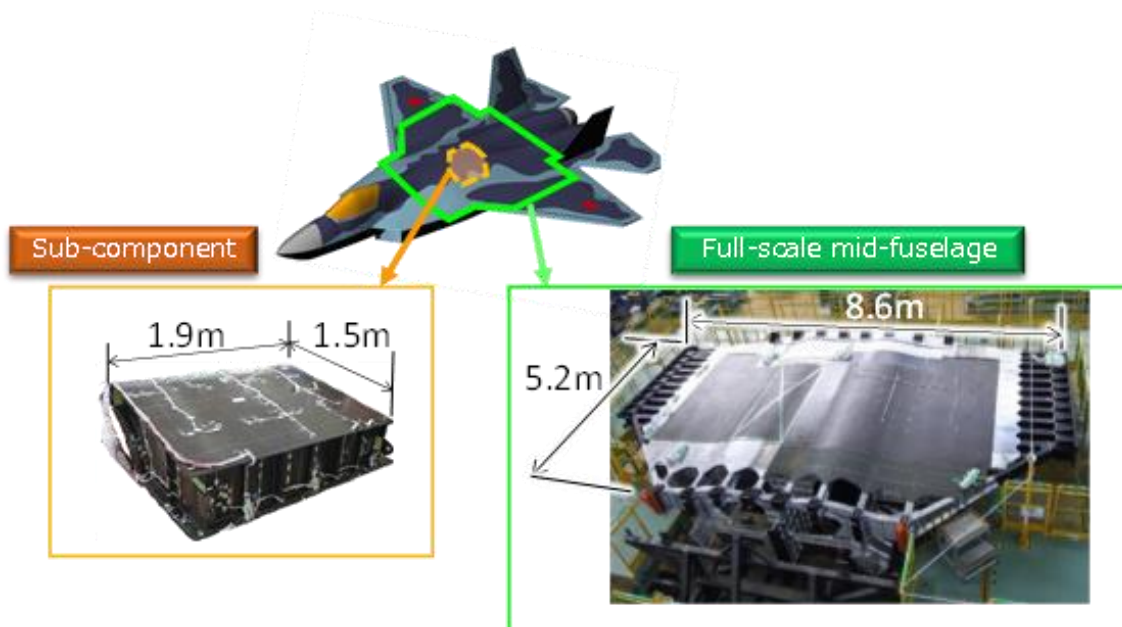


Figure 5.2-1.

6. MISCELLANEOUS

6.1 Lightning Strike Damage of CF/epoxy Composite Laminates with Conductive Polymer Layers

Tomohiro Yokozeki¹

¹The University of Tokyo, Japan

Carbon fiber reinforced plastics (CFRPs) are prone to severe damages by lightning strikes due to their low electrical conductivity. Current lightning strike protection (LSP) technology generally consists of metal foils/films on the surface of composite airframe structures. The present work aims to introduce all polymeric conductive layer for LSP of CFRP structures. Intrinsic conductive polymer i.e. Polyaniline (PANI) is used to make a thermosetting polymer mixture. CFRPs coated with this electrically conductive, all polymeric layer was tested against simulated lightning strike. It has been shown that PANI-LSP specimens dissipated the lightning current effectively and provided enough residual mechanical properties of CFRPs.

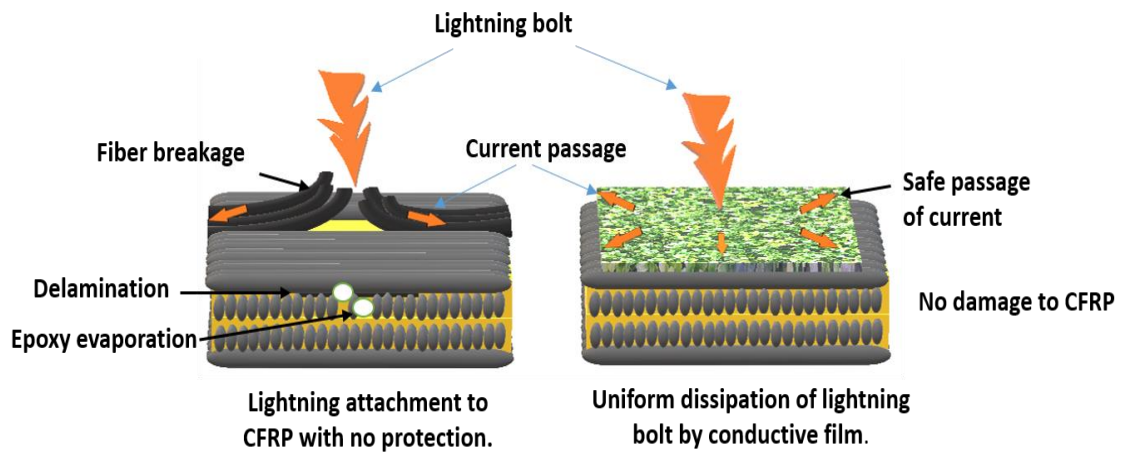


Figure 6.1-1.

6.2 Effect of Plate Thickness and Paint on Lightning Strike Damage of Aluminum Alloy Sheet

Takao Okada ¹, Hiromitsu Miyaki ¹, Yoshiyasu Hirano ¹

¹Japan Aerospace Exploration Agency, Tokyo, Japan

Aircraft usually avoid areas associated with lightning. However, when such areas are directly along the take off or landing path and cannot be avoided without delay, there is a risk of lightning strike during flight. After an aircraft has been hit by lightning, maintenance technicians have to identify the lightning entry and exit points and conduct any necessary repairs before the next flight, and must perform these tasks as quickly as possible to minimize disruption to operations. Composite materials have low conductivity compared to conventional metal structures and so sustain greater lightning strike damage, and there has been much research into the lightning resistance of composites. On the other hand, metallic material has high conductivity and it is known that the damage is small comparing to composite material. However, the knowledge concerning about the lightning strike damage on metallic material contributes to minimize the damage size and the duration of repair.

The effect of plate thickness on lightning strike damage for 2024-T3 aluminum alloy sheet is evaluated. Dimension of the sheet is 150 mm X 150 mm, and two types of the thickness 1.27 and 2.03 mm are prepared.

Modified wave form A of SAE APR 5412 B is utilized for evaluation. Two levels of peak current, 40 and 100 kA, are used. The effect of paint on the surface is also evaluated. Test result shows that the surface of the specimen is melt by the high heat input during the lightning strike and the area can be distinguished by the appearance. In addition, the result shows that the lightning strike damage on the specimen with paint has smaller damage comparing to that on the specimen without paint, and then the paint acts as insulator.

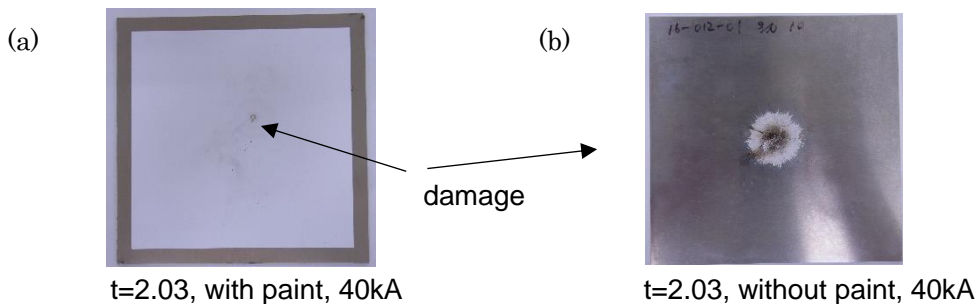


Figure 6.2-1. Lightning strike damage on 2024-T3 aluminum alloy.
(a) with paint, (b) without paint

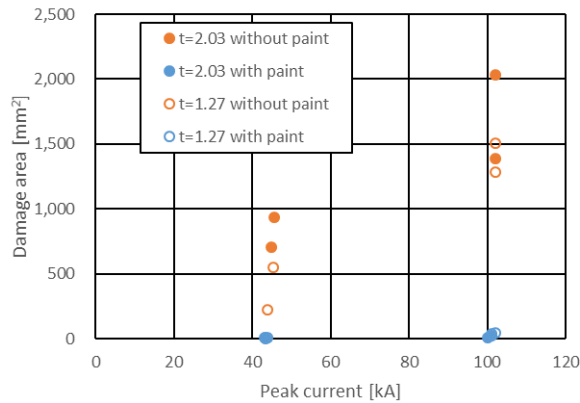


Figure 6.2-2. Effect of plate thickness and paint on lightning strike damage

ACKNOWLEDGEMENTS

The editors appreciated the members of the ICAF national committee of Japan Society for Aeronautical and Space Sciences and other participants in the committee, for their contribution in preparation of this national review and contributing discussion in the committee.